

Article

Approximating isoneutral ocean transport via the Temporal Residual Mean

Andrew L. Stewart ^{1,†,‡}  *

¹ Department of Atmospheric and Oceanic Sciences, University of California, Los Angeles, CA 90095, USA; astewart@atmos.ucla.edu

* Correspondence: astewart@atmos.ucla.edu

Version September 25, 2019 submitted to Fluids

Abstract: Ocean volume and tracer transports are commonly computed on density surfaces because doing so approximates the semi-Lagrangian mean advective transport. The resulting density-averaged transport can be related approximately to Eulerian-averaged quantities via the temporal residual mean (TRM), valid in the limit of small isopycnal height fluctuations. This article builds on a formulation of the TRM for volume fluxes within Neutral Density surfaces, [the “NDTRM”, 1], selected because Neutral Density surfaces are constructed to be as neutral as possible while still forming well-defined surfaces. This article derives a TRM, referred to as the “Neutral TRM” (NTRM), that approximates volume fluxes within surfaces whose vertical fluctuations are defined directly by the neutral relation. The purpose of the NTRM is to more closely approximate the semi-Lagrangian mean transport than the NDTRM, because the latter introduces errors associated with differences between the instantaneous state of the modeled/observed ocean and the reference climatology used to assign the Neutral Density variable. It is shown that the NDTRM collapses to the NTRM in the limiting case of a Neutral Density variable defined with reference to the Eulerian-mean salinity, potential temperature and pressure, rather than an external reference climatology, and therefore that the NTRM approximately advects this density variable. This prediction is verified directly using output from an idealized eddy-resolving numerical model. The NTRM therefore offers an efficient and accurate estimate of modeled semi-Lagrangian mean transports without reference to an external reference climatology, but requires that a Neutral Density variable be computed once from the model’s time-mean state in order to estimate isopycnal and diapycnal components of the transport.

Keywords: isoneutral transport; Temporal Residual Mean; overturning circulation; Neutral Density

1. Introduction

Accurate quantification of the ocean’s meridional overturning circulation (MOC) is required to infer oceanic transport of heat and other tracers around the globe [2,3]. It has been common practice for decades to quantify the MOC in some form of density coordinate system [e.g. 4–9]. Because flow in the ocean interior is quasi-adiabatic, this approach approximately corresponds to taking a semi-Lagrangian mean, which in turn approximates the full Lagrangian-mean transport [10]. In comparison to an MOC based on mass fluxes averaged at constant depth, the semi-Lagrangian mean transport velocity contains an additional “eddy” transport, essentially a generalized Stokes drift [11]. This eddy transport is particularly important in the Southern Ocean [12–14], and therefore forms a key component of recent conceptual models of the global overturning circulation [15–20].

The separation of the semi-Lagrangian mean transport into mean and eddy components can be made explicit via the Temporal Residual Mean (TRM) formulation, which is valid in the asymptotic limit of small isopycnal height fluctuations [10,21,22]. In this article we use “TRM” to refer to the

35 TRM-II [22], but it is straightforward to extend our results to the TRM-I; the distinction between the
 36 two is discussed by [23]. The TRM relates the eddy component of the transport to correlations between
 37 the lateral velocity (u) and density (γ) fields, and thereby allows an estimate of the semi-Lagrangian
 38 mean transport streamfunction to be computed from Eulerian-averaged quantities. The resulting
 39 TRM streamfunction Ψ advects the density variable γ in the following sense: in the absence of
 40 non-conservative sources and sinks of γ , the density γ is materially conserved following the transport
 41 velocity defined by Ψ , up to a consistent asymptotic order in the amplitude of the isopycnal height
 42 fluctuations [23].

43 This article builds upon the Neutral Density Temporal Residual Mean (NDTRM) formulation [1,
 44 hereafter ST15]. In ST15's formulation the Neutral Density variable of [24], referred to henceforth as
 45 γ^{JM97} , was the advected density variable. However, the transport streamfunction Ψ was calculated
 46 from correlations between the lateral velocity, salinity, potential temperature and pressure. This
 47 approach bears the following advantages: (i) The NDTRM can be applied in regions where potential
 48 density referenced to any level becomes vertically non-monotonic somewhere in the water column
 49 (e.g. parts of the high-latitude oceans). (ii) The NDTRM circumvents the computational expense of
 50 calculating Neutral Density globally at every model time step, as would be required to compute the
 51 semi-Lagrangian mean transport velocity, either exactly or via the TRM. (iii) More fundamentally,
 52 isopycnals of Neutral Density are more closely aligned with the local neutral tangent plane, in a
 53 global sense, than any potential density variable [24]. ST15 compared various formulations of the
 54 TRM, and verified that higher-order approximations to the NDTRM most closely approximated the
 55 volume fluxes computed exactly within γ^{JM97} surfaces from numerical model output. The NDTRM
 56 therefore offers a computationally efficient estimate of isopycnal volume fluxes within surfaces of a
 57 stably stratified density variable that has been used widely in quantifications of the ocean's global
 58 overturning circulation [e.g. 6,25].

59 In this article we pursue the related but distinct goal of approximating the semi-Lagrangian
 60 mean transport using vertical fluctuations defined directly by the neutral relationship [26], which we
 61 refer to as local Neutral Surfaces. In pursing this goal we make the assumption that it is these local
 62 Neutral Surfaces that should heave vertically under perfectly adiabatic motions [27,28], and as such
 63 they are best suited for calculation of the semi-Lagrangian mean transport [10]. The validity of these
 64 assumptions is discussed further in §5. In §2 we summarize relevant background literature, specifically
 65 the formulation of the TRM [21,22] and the derivation of the NDTRM by ST15. In §3 we derive a
 66 form of the TRM, which we refer to as the "Neutral TRM" (NTRM), that approximates volume fluxes
 67 within local Neutral Surfaces. However, Neutral Surfaces are globally ill-defined [29]. This means
 68 that isoneutral volume fluxes cannot be associated with a globally-defined, stably-stratified density
 69 variable [30], which is desireable for quantifying global circulation and water mass transformation
 70 [6,25,31]. This motivates us to return to the NDTRM, which is associated with a globally-defined
 71 density variable, and consider the special case of a Neutral Density constructed with reference to the
 72 Eulerian-mean salinity, potential temperature and pressure. We show that in this case, the NDTRM
 73 reduces to the NTRM to a consistent asymptotic order in the amplitude of the isopycnal height
 74 fluctuations. This implies that the NTRM advects a Neutral Density variable defined with respect
 75 to the Eulerian-mean ocean state, again up to a consistent asymptotic order in the amplitude of the
 76 isopycnal height fluctuations. In §4 we evaluate our results using idealized numerical simulations, and
 77 verify that the NTRM and NDTRM more closely approximate volume fluxes within Neutral Density
 78 surfaces constructed based on the model's mean state and based on an independent reference dataset,
 79 respectively. Finally, in §5 we summarize and provide concluding remarks.

80 2. Approximating volume fluxes within Neutral Density surfaces

81 There is a substantial existing literature on the subjects of Neutral Surfaces and the TRM
 82 approximation [e.g. 21,22,24,26]. To achieve a self-contained presentation, this section summarizes
 83 relevant concepts from this literature, and from the derivation of the NDTRM by ST15.

84 2.1. The Temporal Residual Mean (TRM) streamfunction

85 The TRM transport is fundamentally related to fluctuations of material or quasi-material surfaces,
 86 typically defined in terms of a density/buoyancy variable [21,22]. While it is impractical to quantify
 87 the Lagrangian-mean transport of fluid parcels in the ocean in the most general sense [32], a close
 88 approximation can be obtained by exploiting vertically stratified, quasi-material surfaces, commonly
 89 defined via a suitable density or buoyancy variable [23]. Consider a series of vertically monotonic,
 90 temporally-evolving, quasi-material surfaces identified by a label γ_0 , currently not assigned any
 91 physical meaning. We define a streamfunction Ψ at any horizontal point (x_0, y_0) on surface γ_0 as the
 92 lateral mass flux above that surface,

$$93 \quad \Psi(x_0, y_0, \gamma_0) = \overline{\int_{z=z_0(x_0, y_0, \gamma_0, t)}^{z=0} \mathbf{u} dz}, \quad (1)$$

94 where $\mathbf{u} = (u, v)$ is the horizontal velocity vector and we have assumed a flat ocean surface ($z = 0$) for
 95 simplicity. The overline indicates a time average, but could be interpreted more broadly as an average
 96 over an ensemble of realizations of the flow [33].

97 The TRM approximates the mass flux defined in (1) under the assumption of small fluctuations in
 98 the quasi-material surfaces, *i.e.* $z_0 = \bar{z}_0 + z'_0$ with $z'_0 = \mathcal{O}(\varepsilon)$ assumed to be asymptotically small. Here
 99 ε may be interpreted as the magnitude of the surface fluctuation relative to some vertical length scale
 100 such as the ocean depth H , so $\varepsilon = z'_0/H \ll 1$. Using Taylor expansions of (1), it may be shown [*e.g.*
 101 1,22] that Ψ may be approximated in Eulerian coordinates as a sum of mean and “eddy” components,
 102 defined as

$$103 \quad \Psi(x_0, y_0, \bar{z}_0) = \bar{\Psi} + \Psi^*, \quad (2a)$$

$$104 \quad \bar{\Psi} = \int_{\bar{z}_0}^0 \bar{\mathbf{u}} dz, \quad (2b)$$

$$105 \quad \Psi^* = -\overline{\mathbf{u}'(\bar{z}_0) z'_0} - \frac{1}{2} \bar{\mathbf{u}}_z(\bar{z}_0) \overline{z'_0}^2 + \mathcal{O}(\varepsilon^3). \quad (2c)$$

107 Here, and henceforth in this manuscript, the rules of Reynolds averaging are assumed to apply unless
 108 otherwise stated, *i.e.* $\bar{\bullet} = \bullet$ and $\overline{\bullet} = 0$ for any \bullet . Note that $\bar{\Psi}$ and Ψ^* are streamfunctions in the sense
 109 that their curl is equal to a non-divergent velocity field.

110 To write (2a) in terms of only mean quantities, and therefore to create a useful approximation to
 111 the ocean’s Lagrangian-mean velocities, we require a suitable approximation to the surface fluctuations
 112 z'_0 . Correlations of quantities such as $\overline{\mathbf{u}' z'_0}$ and $\overline{z'_0}^2$ are not routinely provided as output from ocean
 113 models formulated in Eulerian vertical coordinate systems, partly due to the ambiguity in the definition
 114 of z_0 , so instead z'_0 is typically related to Eulerian fluctuations of thermodynamic variables [*e.g.* 1,23].
 115 For a vertically monotonic label γ , we can further Taylor-expand our continuum of labels γ to obtain
 116 an $\mathcal{O}(\varepsilon^2)$ approximation to z'_0 [22,23],

$$117 \quad \gamma'(\bar{z}_0) = -z'_0 \bar{\gamma}_z(\bar{z}_0) + \mathcal{O}(\varepsilon^2), \quad (3)$$

118 allowing us to express the TRM “eddy” streamfunction in terms of purely Eulerian variables,

$$119 \quad \Psi^*(x_0, y_0, \bar{z}_0) = \frac{\overline{\mathbf{u}' \gamma'}}{\bar{\gamma}_z} - \frac{1}{2} \frac{\bar{\mathbf{u}}_z}{\bar{\gamma}_z^2} \overline{\gamma'}^2 + \mathcal{O}(\varepsilon^3). \quad (4)$$

120 Note that all variables on the right-hand side are evaluated at the mean surface elevation \bar{z}_0 .
 121 Additionally, note that the $\mathcal{O}(\varepsilon^3)$ error terms on the right-hand side of (4) differ from those on the
 122 right-hand side of (2c); additional $\mathcal{O}(\varepsilon^3)$ terms have been included in the error term following the
 123 substitution for γ' using (3). In the interest of brevity, throughout this article we will write the error

124 terms in terms of their lowest-order dependence on the relevant asymptotically small parameters
 125 without specifically identifying when the mathematical definition of the error terms has changed.

126 In the form of equation (4), the TRM streamfunction is in principle straightforward to calculate
 127 from ocean model output if we associate γ with, for example, potential density or Neutral Density [24],
 128 discussed in §2.2]. However, potential density surfaces are not particularly neutral, while the Neutral
 129 Density variable of [24] is too computationally expensive for practical use in ocean models [1].

130 *2.2. The Neutral Density Temporal Residual Mean (NDTRM)*

131 ST15 derived alternative expressions to (3) for the vertical fluctuations (z'_0) of isopycnals of a
 132 Neutral Density variable (γ). These expressions contain no explicit dependence on γ itself, and so
 133 circumvent the need to explicitly compute a Neutral Density variable in order to construct the TRM.
 134 Here we briefly summarize the portions of this derivation and the resulting expressions for z'_0 required
 135 in §3.

136 The Neutral Density variable of [24] is assigned based on geographically distributed reference
 137 casts. Each reference cast is pre-labeled with Neutral Density γ as a function of depth, such that the
 138 cast potential temperature, salinity and pressure may be written as $\theta_c(\gamma)$, $S_c(\gamma)$ and $p_c(\gamma)$, respectively.
 139 To assign a Neutral Density label to a given point in space and time, the potential temperature (θ_0),
 140 salinity (S_0) and pressure (p_0) at that point are compared with a nearby reference cast. Specifically, the
 141 assigned value of γ is that which satisfies the “discrete neutral relation”, which ST15 wrote as

$$142 \quad (S_c(\gamma) - S_0) \beta_m - (\theta_c(\gamma) - \theta_0) \alpha_m = \mathcal{O}(\Delta^3). \quad (5)$$

144 This relation states that water parcels with properties (S_0, θ_0, p_0) and $(S_c(\gamma), \theta_c(\gamma), p_c(\gamma))$ would have
 145 equal densities if both were moved adiabatically and isentropically to the mid-point pressure between
 146 the two parcels. Here β_m and α_m are short-hands for

$$147 \quad \beta_m \equiv \beta(S_m, \theta_m, p_m), \quad \alpha_m \equiv \alpha(S_m, \theta_m, p_m), \quad (6)$$

148 *i.e.*, the saline contraction and thermal expansion coefficients evaluated at the thermodynamic
 149 mid-point (S_m, θ_m, p_m) , which is defined as

$$150 \quad S_m(\gamma) \equiv (S_0 + S_c(\gamma))/2, \quad (7a)$$

$$151 \quad \theta_m(\gamma) \equiv (\theta_0 + \theta_c(\gamma))/2, \quad (7b)$$

$$152 \quad p_m(\gamma) \equiv (p_0 + p_c(\gamma))/2. \quad (7c)$$

154 The small parameter Δ measures deviations of the properties (S_0, θ_0, p_0) from the mid-values
 155 (S_m, θ_m, p_m) . See [1] for further details on the definition of Δ and the asymptotic derivation of (5).

156 To derive an expression for the vertical fluctuations of a Neutral Density surface, ST15 considered
 157 the semi-Lagrangian evolution of the thermodynamic properties on such a surface, *i.e.* $S_0 = S(z_0(t), t)$,
 158 $\theta_0 = \theta(z_0(t), t)$, and $p_0 = p(z_0(t), t)$. They then posed Taylor expansions of (5) in terms of ε and Δ , *e.g.*

$$159 \quad S(z_0(t), t) = \overline{S(\bar{z}_0, t)} + \overline{S_z(\bar{z}_0, t)} z'_0 + S'(\bar{z}_0, t) + \mathcal{O}(\varepsilon^2). \quad (8)$$

160 where $S'(\bar{z}_0, t) = S(\bar{z}_0, t) - \overline{S(\bar{z}_0, t)}$ is the Eulerian fluctuation of the salinity at $z = \bar{z}_0$.

161 In this article we restrict our attention to the Boussinesq case for simplicity. This effectively
 162 corresponds to replacing p_0 , p_c and p_m by z_0 , z_c and z_m , where z_c is the depth of the Neutral Density

163 label γ on the reference cast and $z_m = \frac{1}{2}(z_0 + z_c)$. In this case, the highest-order NDTRM approximation
 164 to z'_0 (the “NDTRM2” of ST15) is

$$\begin{aligned}
 165 \quad z'_{\text{NDTRM2}} & \left\{ -\bar{S}_z \hat{\beta}_m + \bar{\theta}_z \hat{\alpha}_m + (S_c - \bar{S}) \left[\frac{1}{2} \bar{S}_z \frac{\partial \hat{\beta}_m}{\partial \bar{S}_m} + \frac{1}{2} \bar{\theta}_z \frac{\partial \hat{\beta}_m}{\partial \bar{\theta}_m} + \frac{1}{2} \frac{\partial \hat{\beta}_m}{\partial \bar{z}_m} \right] \right. \\
 166 \quad & \left. - (\theta_c - \bar{\theta}) \left[\frac{1}{2} \bar{S}_z \frac{\partial \hat{\alpha}_m}{\partial \bar{S}_m} + \frac{1}{2} \bar{\theta}_z \frac{\partial \hat{\alpha}_m}{\partial \bar{\theta}_m} + \frac{1}{2} \frac{\partial \hat{\alpha}_m}{\partial \bar{z}_m} \right] \right\} \\
 167 \quad & = - \left\{ -S' \hat{\beta}_m + \theta' \hat{\alpha}_m + (S_c - \bar{S}) \left[\frac{1}{2} S' \frac{\partial \hat{\beta}_m}{\partial \bar{S}_m} + \frac{1}{2} \theta' \frac{\partial \hat{\beta}_m}{\partial \bar{\theta}_m} \right] - (\theta_c - \bar{\theta}) \left[\frac{1}{2} S' \frac{\partial \hat{\alpha}_m}{\partial \bar{S}_m} + \frac{1}{2} \theta' \frac{\partial \hat{\alpha}_m}{\partial \bar{\theta}_m} \right] \right\} \\
 168 \quad & \quad + \mathcal{O}(\Delta^3, \varepsilon^2). \quad (9) \\
 169 \\
 170
 \end{aligned}$$

171 Here we use shorthand notation for the Eulerian-mean salinity and potential temperature at constant
 172 height,

$$173 \quad \bar{S}(\bar{z}_0) \equiv \bar{S}(\bar{z}_0, t), \quad \bar{\theta}(\bar{z}_0) \equiv \bar{\theta}(\bar{z}_0, t), \quad (10)$$

174 and for the haline contraction and thermal expansion coefficients evaluated as functions of
 175 Eulerian-mean properties,

$$176 \quad \hat{\beta}_m \equiv \beta(\bar{S}_m, \bar{\theta}_m, \bar{z}_m), \quad \hat{\alpha}_m \equiv \alpha(\bar{S}_m, \bar{\theta}_m, \bar{z}_m). \quad (11)$$

177 Equation (9) approximately relates the Neutral Surface height fluctuations to Eulerian fluctuations of S
 178 and θ , in analogy with (3). By excluding terms from (9), ST15 derived lower-order approximations to
 179 z'_0 , referred to as the “NDTRM1”,

$$180 \quad z'_{\text{NDTRM1}} = -\frac{S' \hat{\beta}_m - \theta' \hat{\alpha}_m}{\bar{S}_z \hat{\beta}_m - \bar{\theta}_z \hat{\alpha}_m} + \mathcal{O}(\Delta^3, \varepsilon^2, \varepsilon \tilde{\Delta}), \quad (12)$$

181 and “NDTRM0”

$$182 \quad z'_{\text{NDTRM0}} = -\frac{S' \hat{\beta} - \theta' \hat{\alpha}}{\bar{S}_z \hat{\beta} - \bar{\theta}_z \hat{\alpha}} + \mathcal{O}(\Delta^3, \tilde{\Delta}^2, \varepsilon^2, \varepsilon \tilde{\Delta}), \quad (13)$$

183 where we define

$$184 \quad \hat{\beta} \equiv \beta(\bar{S}, \bar{\theta}, \bar{z}_0), \quad \hat{\alpha} \equiv \alpha(\bar{S}, \bar{\theta}, \bar{z}_0) \quad (14)$$

185 in analogy with (11). For brevity we omit complete expressions for the NDTRM streamfunctions,
 186 derived by substituting (9)–(13) into (2a), and a discussion of the evaluation of the “cast” terms S_c and
 187 θ_c ; we refer the reader to ST15 for information on such specifics of the NDTRM.

188 These expressions differ from those given by ST15 via the introduction of an additional small
 189 parameter, $\tilde{\Delta}$, that measures deviations of the Eulerian mean properties, \bar{S} and $\bar{\theta}$, from the cast
 190 properties, S_c and θ_c . Thus, conceptually, the three small parameters in (9)–(13) are related via
 191 $\Delta \sim \tilde{\Delta} + \varepsilon$.

192 3. Approximating volume fluxes within local Neutral Surfaces

193 The Neutral Density variable of [24] (γ^{JM97}) was formulated with the aim of obtaining a
 194 density-like variable whose surfaces lie as parallel as possible to the local neutral tangent plane
 195 everywhere in the ocean. However, due to the ocean’s equation of state, is not possible to construct
 196 such a variable exactly [29,30]. Thus in general the vertical fluctuations of Neutral Density surfaces
 197 differ from fluctuations of local Neutral Surfaces [34]. In §1 we posited that local Neutral Surfaces
 198 are best suited to estimating semi-Lagrangian mean transport, and therefore also to formulating
 199 the TRM, because adiabatic flows are constrained to follow these surfaces. The validity of these
 200 assumptions is discussed further in §5.

201 In this section we aim to formulate a TRM that approximates fluxes along local Neutral Surfaces
 202 as closely as possible (the NTRM). We first derive an approximation to the vertical fluctuations of
 203 local Neutral Surfaces, denoted z'_{NS} for comparison with the NDTRM approximations to z'_0 given in
 204 §2. This approximation alone yields an incomplete TRM because the resulting streamfunction (2a) is
 205 not associated with a globally-defined set of surfaces (*i.e.* γ). To circumvent this issue we consider a
 206 Neutral Density variable γ^{mean} whose reference dataset (*i.e.* S_c , θ_c and p_c) is chosen to be the local
 207 Eulerian-mean thermodynamic properties (*i.e.* \bar{S} , $\bar{\theta}$ and \bar{z}). For such a Neutral Density variable the
 208 NDTRM reduces to the NTRM, up to the same asymptotic order in ε , which implies that the NTRM
 209 does in fact advect a globally-defined density variable, γ^{mean} . We also show that the NTRM coincides
 210 with a TRM derived based on fluctuations of surfaces of locally-referenced potential density, up to the
 211 same asymptotic order in ε .

212 *3.1. Vertical fluctuations of local Neutral Surfaces*

213 Consider a local Neutral Surface with instantaneous height $z = z_0(t)$ at a fixed horizontal location
 214 (x_0, y_0). To simplify our presentation we will drop all dependence on horizontal location in what
 215 follows. We define the time-evolution of $z_0(t)$ via the semi-Lagrangian neutral relationship [26],

$$216 \quad \beta \delta S(z_0(t), t) - \alpha \delta \theta(z_0(t), t) = 0, \quad (15)$$

217 where δS and $\delta \theta$ denote infinitesimal changes in the salinity and potential temperature on the surface.
 218 Both β and α are themselves evaluated at the local salinity $S(z_0(t), t)$, potential temperature $\theta(z_0(t), t)$
 219 and pressure $p(z_0(t), t)$. Dividing by an infinitesimal unit of time δt , equation (15) may be expanded
 220 to describe the time evolution of z_0 ,

$$221 \quad \left[\beta \frac{\partial S}{\partial z}(z_0, t) - \alpha \frac{\partial \theta}{\partial z}(z_0, t) \right] \frac{dz_0}{dt} = - \left[\beta \frac{\partial S}{\partial t}(z_0, t) - \alpha \frac{\partial \theta}{\partial t}(z_0, t) \right]. \quad (16)$$

222 We now use (16) to derive a relationship between the Neutral Surface height fluctuations $z'_0 =$
 223 $z_0(t) - \bar{z}_0$ and the Eulerian fluctuations of S and θ . Note that fluctuations of S and θ may not only
 224 be associated with vertical heaving of Neutral Surfaces; they may also result from lateral stirring
 225 of property gradients along Neutral Surfaces. To simplify the presentation we assume that the
 226 magnitudes of both vertical heaving-induced and lateral stirring-induced property fluctuations are
 227 small and characterized by the same small parameter ε . A caveat to this assumption is that even
 228 outside of the ocean's surface and bottom boundary layers there may be a non-negligible influence of
 229 surface buoyancy fluxes [35]. For further discussion of these points and a rationalization of the small
 230 parameter ε , the reader is referred to ST15.

231 By posing Taylor expansions of β and α as *e.g.*

$$232 \quad \beta(S(z_0(t), t), \theta(z_0(t), t), z_0(t)) = \beta(\bar{S}(\bar{z}_0), \bar{\theta}(\bar{z}_0), \bar{z}_0) + \mathcal{O}(\varepsilon) = \hat{\beta} + \mathcal{O}(\varepsilon), \quad (17)$$

233 we can approximate (16) as

$$234 \quad \left[\hat{\beta} \frac{\partial \bar{S}}{\partial z}(\bar{z}_0, t) - \hat{\alpha} \frac{\partial \bar{\theta}}{\partial z}(\bar{z}_0, t) \right] \frac{dz'_0}{dt} = - \left[\hat{\beta} \frac{\partial S'}{\partial t}(\bar{z}_0, t) - \hat{\alpha} \frac{\partial \theta'}{\partial t}(\bar{z}_0, t) \right] + \mathcal{O}(\varepsilon^2). \quad (18)$$

235 Finally, integrating (18) with respect to t yields an expression for the local Neutral Surface height
 236 fluctuation, which we denote as z'_{NS} , in terms of S' and θ' ,

$$237 \quad \left(\hat{\beta} \frac{\partial \bar{S}}{\partial \bar{z}_0} - \hat{\alpha} \frac{\partial \bar{\theta}}{\partial \bar{z}_0} \right) z'_{\text{NS}} = - \left(\hat{\beta} S' - \hat{\alpha} \theta' \right) + \mathcal{O}(\varepsilon^2). \quad (19)$$

238 Note that the constant of integration vanishes between (18) and (19) because by definition, $\bar{z}'_0 = \bar{S}' =$
 239 $\bar{\theta}' = 0$. Substituting (19) into (2a)–(2c) yields the following expression for the NTRM streamfunction,

240

$$241 \quad \Psi(x_0, y_0, \bar{z}_0) = \int_{\bar{z}_0}^0 \bar{u} dz + \frac{\hat{\beta} \bar{u}' \bar{S}' - \hat{\alpha} \bar{u}' \bar{\theta}'}{\hat{\beta} \partial_{\bar{z}_0} \bar{S} - \hat{\alpha} \partial_{\bar{z}_0} \bar{\theta}} - \frac{1}{2} \frac{\bar{u}_z(\bar{z}_0)}{\left(\hat{\beta} \partial_{\bar{z}_0} \bar{S} - \hat{\alpha} \partial_{\bar{z}_0} \bar{\theta} \right)^2} \left(\hat{\beta}^2 \bar{S}'^2 - 2\hat{\beta}\hat{\alpha} \bar{S}' \bar{\theta}' + \hat{\alpha}^2 \bar{\theta}'^2 \right) + \mathcal{O}(\varepsilon^3). \quad (20)$$

242

243 Note that in applying (20) we are free to select \bar{z}_0 , for example to coincide with a model vertical grid
 244 level. Equation (19) then approximates the vertical fluctuations of a local Neutral Surface $z_0(t)$ whose
 245 mean elevation is \bar{z}_0 , and (20) approximates the transport above $z = \bar{z}_0$.

246 3.2. Connection to the Neutral Density Temporal Residual Mean (NDTRM)

247 While the NTRM streamfunction (20) approximates the semi-Lagrangian mean transport, in
 248 isolation it does not quantify isopycnal/diapycnal fluxes because we have not yet associated it with a
 249 globally-defined set of surfaces (*i.e.* γ). It therefore does not advect a density variable, and the fluxes
 250 cannot be partitioned into adiabatic and diabatic components [*e.g.* 23]. We therefore now consider
 251 whether the NDTRM, which is associated with a globally-defined density variable (*e.g.* γ^{JM97}), can be
 252 adapted to more closely approximate the fluxes within local Neutral Surfaces.

253 We first note that there is a close similarity between our equations for the vertical fluctuations of
 254 local Neutral Surfaces, (19), and the vertical fluctuations of Neutral Density surfaces, (9)–(13). Indeed,
 255 (19) is identical to the *lowest*-order form of the NDTRM, the NDTRM0 (13), except for the differing
 256 asymptotic order of the error terms,

257

$$z'_{\text{NDTRM0}} = z'_{\text{NS}} + \mathcal{O}(\Delta^3, \tilde{\Delta}^2, \varepsilon \tilde{\Delta}, \varepsilon^2). \quad (21)$$

258 In other words, there are $\mathcal{O}(\Delta^3)$, $\mathcal{O}(\tilde{\Delta}^2)$ and $\mathcal{O}(\varepsilon \tilde{\Delta})$ terms that appear explicitly on the right-hand sides
 259 of (9) and (12), and these terms allow z'_{NDTRM2} and z'_{NDTRM1} to more closely approximate Neutral
 260 Density surface fluctuations than z'_{NDTRM0} . However, by treating these $\mathcal{O}(\Delta^3)$, $\mathcal{O}(\tilde{\Delta}^2)$ and $\mathcal{O}(\varepsilon \tilde{\Delta})$ terms
 261 as error terms in (13) we actually obtain a closer approximation of local Neutral Surface fluctuations
 262 (*i.e.* of (19)).

263 Motivated by this observation, we now seek a hypothetical Neutral Density variable that
 264 eliminates the $\mathcal{O}(\Delta^2)$, $\mathcal{O}(\tilde{\Delta}^2)$ and $\mathcal{O}(\varepsilon \tilde{\Delta})$ terms in the NDTRM. This is achieved by constructing
 265 a Neutral Density variable, referred to as γ^{mean} , using the Eulerian-mean thermodynamic properties
 266 in place of the reference dataset,

267

$$(S_c(\gamma), \theta_c(\gamma), z_c(\gamma)) \rightarrow (\bar{S}(z_r(\gamma)), \bar{\theta}(z_r(\gamma)), z_r(\gamma)). \quad (22)$$

268 Here we have implicitly assumed that the local water column has been pre-labeled with γ based on
 269 the Eulerian-mean thermodynamic properties, and the reference elevation $z_r(\gamma)$ is the elevation in this
 270 water column that has been labeled with Neutral Density γ . The isopycnal fluctuation $z = z_0(t)$ is
 271 therefore defined by the discrete neutral relation (5) in the form

272

$$(\bar{S}(z_r(\gamma)) - S(z_0(t), t)) \beta_m - (\bar{\theta}(z_r(\gamma)) - \theta(z_0(t), t)) \alpha_m = \mathcal{O}(\Delta^3). \quad (23)$$

274 Here β_m and α_m are defined as in (6), but with the thermodynamic mid-point defined as

275

$$S_m(z_0(t), t, \gamma) \equiv [S(z_0(t), t) + \bar{S}(z_r(\gamma))] / 2, \quad (24a)$$

276

$$\theta_m(z_0(t), t, \gamma) \equiv [\theta(z_0(t), t) + \bar{\theta}(z_r(\gamma))] / 2, \quad (24b)$$

277

$$z_m(t, \gamma) \equiv (z_0(t) + z_r(\gamma)) / 2. \quad (24c)$$

278

Note that the transformation defined by (22) and (24a)–(24c) does not immediately eliminate the $\mathcal{O}(\Delta^2)$, $\mathcal{O}(\tilde{\Delta}^2)$ and $\mathcal{O}(\varepsilon\tilde{\Delta})$ terms in the NDTRM formulae (9), (12) and (13). Instead, this transformation implies a modified interpretation of Δ and $\tilde{\Delta}$. We now define $\tilde{\Delta}$ as a measure of the difference between the mean isopycnal elevation \bar{z}_0 and the mean mid-point elevation \bar{z}_m , or equivalently between \bar{z}_0 and z_r , compared to a dynamical scale height H , for example the ocean depth. Via Taylor expansions of $\bar{S}(\bar{z}_0)$ and $\bar{\theta}(\bar{z}_0)$, e.g.,

$$\bar{S}(\bar{z}_0) = \bar{S}(z_r) + (\bar{z}_0 - z_r) \frac{\partial \bar{S}}{\partial \bar{z}_0}(z_r) + \mathcal{O}(\tilde{\Delta}^2) \quad (25)$$

it follows that $\tilde{\Delta}$ also measures deviations of \bar{S} and $\bar{\theta}$ from \bar{S}_m and $\bar{\theta}_m$, or equivalently from $\bar{S}(z_r(\gamma))$ and $\bar{\theta}(z_r(\gamma))$. It then follows from (8) that again $\Delta \sim \tilde{\Delta} + \varepsilon$, where Δ measures differences between $(S(z_0(t), t), \theta(z_0(t), t), z_0(t))$ and $(S_m(z_0(t), t, \gamma), \theta_m(z_0(t), t, \gamma), z_m(t, \gamma))$.

We have now established that the transformation described by (22) and (24a)–(24c) leaves the NDTRM formulae (9), (12) and (13) largely unchanged, but modifies the interpretation of the $\mathcal{O}(\Delta^2)$, $\mathcal{O}(\tilde{\Delta}^2)$ and $\mathcal{O}(\varepsilon\tilde{\Delta})$ error terms. To approach the NTRM, we now demonstrate that

$$\tilde{\Delta} \sim \varepsilon. \quad (26)$$

This implies that the difference (Δ) between the “parcel” properties on the heaving Neutral Density surface and the properties of the reference “cast” (consisting of the Eulerian-mean thermodynamic properties) necessarily scales with the amplitude (ε) of the isopycnal height fluctuations in the limit $\varepsilon \rightarrow 0$. To derive (26), we first note that the reference elevation must approach \bar{z}_0 in the limit of vanishingly small ε , i.e. $z_r(\gamma) \rightarrow \bar{z}_0$ as $\varepsilon \rightarrow 0$, because in this limit $z_0(t) \rightarrow \bar{z}_0$, and the (stationary) isopycnal must satisfy the neutral relation with itself. We therefore write $z_r = \bar{z}_0 + \delta z_r$, where $\delta z_r = \mathcal{O}(\tilde{\Delta})$ by definition, and seek a relationship between δz_r and ε by posing a Taylor expansion of (23) in terms of ε and $\tilde{\Delta}$. First, we note that the midpoint thermodynamic properties can be written as

$$S_m = \bar{S} + \mathcal{O}(\varepsilon, \tilde{\Delta}), \quad \theta_m = \bar{\theta} + \mathcal{O}(\varepsilon, \tilde{\Delta}), \quad z_m = \bar{z}_0 + \mathcal{O}(\varepsilon, \tilde{\Delta}), \quad (27)$$

where we have moved all terms in S' , θ' and z'_0 into the error terms on the right-hand sides of these equations. We can write β_m and α_m as

$$\beta_m = \hat{\beta} + \mathcal{O}(\varepsilon, \tilde{\Delta}), \quad \alpha_m = \hat{\alpha} + \mathcal{O}(\varepsilon, \tilde{\Delta}), \quad (28)$$

where $\hat{\beta}$ and $\hat{\alpha}$ are defined as in (14). Substituting (27) and (28) into (23), Taylor expanding $\bar{S}(z_r(\gamma))$ and $\bar{\theta}(z_r(\gamma))$ in terms of δz_r , and Taylor expanding $S(z_0(t), t)$ and $\theta(z_0(t), t)$ as in (8), we obtain

$$\delta z_r \left(\hat{\beta} \frac{\partial \bar{S}}{\partial \bar{z}_0} - \hat{\alpha} \frac{\partial \bar{\theta}}{\partial \bar{z}_0} \right) = \mathcal{O}(\Delta^3, \varepsilon, \varepsilon\tilde{\Delta}, \tilde{\Delta}^2). \quad (29)$$

Noting again that the left-hand side of (29) is $\mathcal{O}(\tilde{\Delta})$ by definition, we conclude that $\delta z_r = \mathcal{O}(\varepsilon)$ and that (26) holds.

Finally, we combine the transformation defined by (22) and (24a)–(24c) with the asymptotic relationships (27), (28) and (26) to obtain the following transformation of the variables in (9), (12) and (13):

$$\Delta \rightarrow \varepsilon, \quad \tilde{\Delta} \rightarrow \varepsilon, \quad (30a)$$

$$\hat{\alpha}_m \rightarrow \hat{\alpha} + \mathcal{O}(\varepsilon), \quad \hat{\beta}_m \rightarrow \hat{\beta} + \mathcal{O}(\varepsilon), \quad (30b)$$

$$S_c \rightarrow \bar{S} + \mathcal{O}(\varepsilon), \quad \theta_c \rightarrow \bar{\theta} + \mathcal{O}(\varepsilon), \quad (30c)$$

$$\bar{S}_m \rightarrow \bar{S} + \mathcal{O}(\varepsilon), \quad \bar{\theta}_m \rightarrow \bar{\theta} + \mathcal{O}(\varepsilon), \quad \bar{z}_m \rightarrow \bar{z}_0 + \mathcal{O}(\varepsilon). \quad (30d)$$

³¹⁴ Substituting (22)–(30c) into (9)–(13), we find that all forms of the NDTRM collapse to the NTRM, to a
³¹⁵ consistent asymptotic order in ε ,

$$\text{316} \quad z'_{\text{NDTRM2}} = z'_{\text{NS}} + \mathcal{O}(\varepsilon^2), \quad (31\text{a})$$

$$\text{317} \quad z'_{\text{NDTRM1}} = z'_{\text{NS}} + \mathcal{O}(\varepsilon^2), \quad (31\text{b})$$

$$\text{318} \quad z'_{\text{NDTRM0}} = z'_{\text{NS}} + \mathcal{O}(\varepsilon^2). \quad (31\text{c})$$

³²⁰ This implies that, to a consistent order in ε , the NTRM advects a Neutral Density variable γ^{mean}
³²¹ constructed via the discrete neutral relation (5), using the Eulerian-mean thermodynamic properties
³²² $(\bar{S}, \bar{\theta}, \bar{z}_0)$ as the reference dataset.

³²³ 3.3. *Equivalence to fluctuations of locally-referenced potential density surfaces*

³²⁴ We now show that our equation (19) for the vertical fluctuations of Neutral Surfaces also coincides
³²⁵ with the fluctuations of surfaces of locally-referenced potential density, to the same order of accuracy in
³²⁶ ε . [36] used a TRM based on locally-referenced potential density fluctuations, but did not demonstrate
³²⁷ its equivalence to fluctuations of local Neutral Surfaces.

³²⁸ We define locally-referenced potential density $\sigma_{\bar{z}_0}$ as the density referenced to the mean height \bar{z}_0 ,

$$\text{329} \quad \sigma_{\bar{z}_0}(z_0(t), t) \stackrel{\text{def}}{=} \rho(S(z_0(t), t), \theta(z_0(t), t), \bar{z}_0). \quad (32)$$

³³⁰ Here ρ is the *in situ* density and $z_0(t)$ is the instantaneous height of the $\sigma_{\bar{z}_0}$ surface whose mean depth
³³¹ is \bar{z}_0 . Below we identify this $\sigma_{\bar{z}_0}$ surface to a consistent order of asymptotic approximation in the
³³² amplitude of the surface height fluctuation, ε .

³³³ Posing Taylor expansions of S and θ following (8), we may expand (32) as

$$\text{334} \quad \sigma_{\bar{z}_0}(z_0(t), t) = \rho(\bar{S}(\bar{z}_0), \bar{\theta}(\bar{z}_0), \bar{z}_0) \left[1 + \left(S'(\bar{z}_0, t) + z'_0(t) \frac{\partial \bar{S}}{\partial z}(\bar{z}_0, t) \right) \beta(\bar{S}(\bar{z}_0), \bar{\theta}(\bar{z}_0), \bar{z}_0) \right. \\ \text{335} \quad \left. - \left(\theta'(\bar{z}_0, t) + z'_0(t) \frac{\partial \bar{\theta}}{\partial z}(\bar{z}_0, t) \right) \alpha(\bar{S}(\bar{z}_0), \bar{\theta}(\bar{z}_0), \bar{z}_0) \right] + \mathcal{O}(\varepsilon^2). \quad (33)$$

³³⁶ ³³⁷ Taking the mean of (33) yields an expression for the semi-Lagrangian-mean locally-referenced potential
³³⁸ density

$$\text{339} \quad \overline{\sigma_{\bar{z}_0}(z_0(t), t)} = \rho(\bar{S}(\bar{z}_0), \bar{\theta}(\bar{z}_0), \bar{z}_0) + \mathcal{O}(\varepsilon^2). \quad (34)$$

³⁴⁰ As z_0 is defined by a surface of constant locally-referenced potential density, it follows that

$$\text{342} \quad \overline{\sigma_{\bar{z}_0}(z_0(t), t)} \equiv \sigma_{\bar{z}_0}(z_0(t), t). \quad (35)$$

Substituting (35) and (34) into (33) eliminates the first two terms in (33) to a consistent order of approximation in ε , and thus (33) reduces to

$$z'_{\text{LRPD}} = z'_{\text{NS}} + \mathcal{O}(\varepsilon^2), \quad (36)$$

³⁴³ where z'_{LRPD} denotes vertical fluctuations of the locally-referenced potential density surface. Therefore,
³⁴⁴ to the same asymptotic order of approximation in ε , the NTRM estimate of isopycnal height fluctuations
³⁴⁵ also coincides with vertical fluctuations of locally-referenced potential density surfaces.

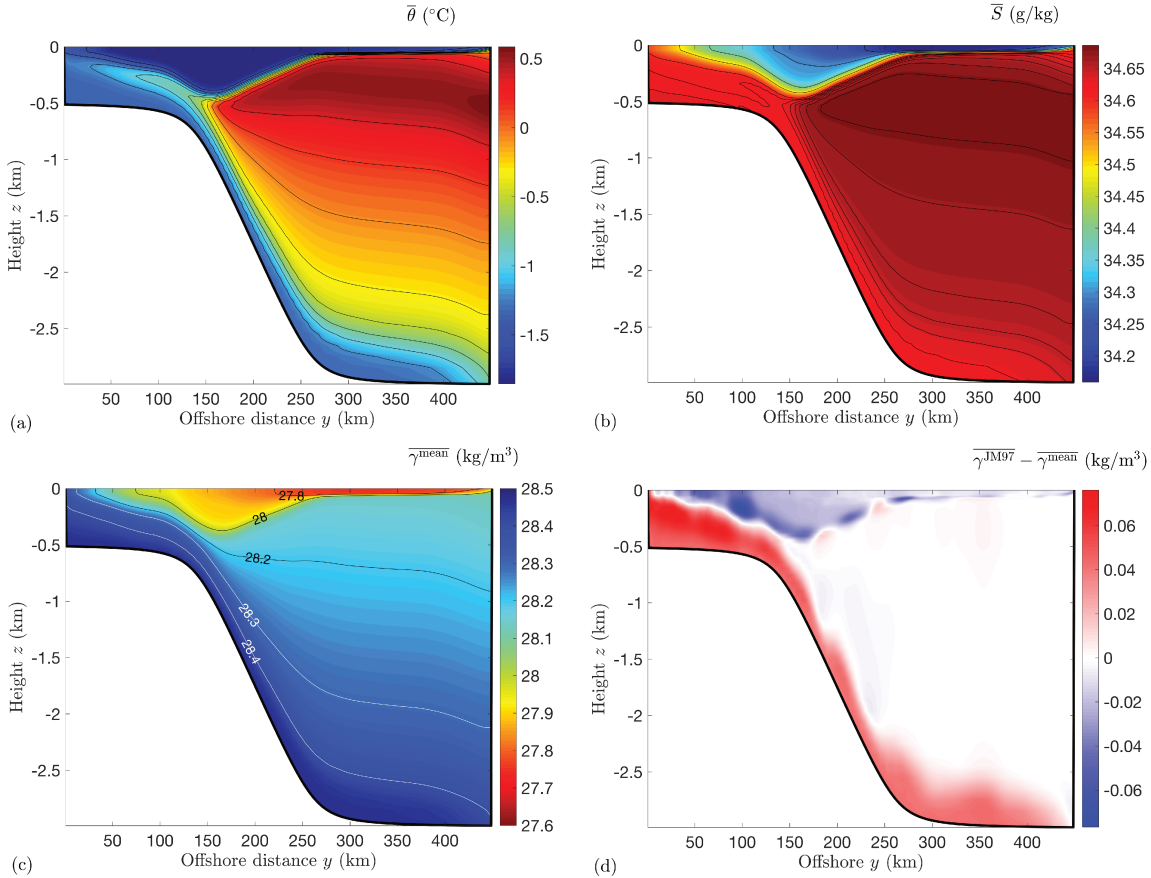


Figure 1. Diagnostics of the mean model state, where averages are taken in time (over 5 years of daily snapshots) and in the along-slope (zonal) direction (400 km distance at ~ 1 km horizontal grid spacing. (a) Potential temperature θ , (b) practical salinity S , (c) Neutral Density constructed based on the model's mean state, which we denote as $\bar{\gamma}^{\text{mean}}$ (see §4), (d) difference between $\bar{\gamma}^{\text{JM97}}$, where $\bar{\gamma}^{\text{JM97}}$ is the Neutral Density calculated using the reference dataset and algorithm of [24], and $\bar{\gamma}^{\text{mean}}$.

346 4. Comparison and assessment using an idealized numerical model

347 The key result of §3 is that the NTRM streamfunction (20) approximates volume fluxes within
 348 local Neutral Surfaces, and advects a Neutral Density variable defined using the Eulerian-mean
 349 thermodynamic properties $(\bar{S}, \bar{\theta}, \bar{z}_0)$ as a reference dataset. An implication of this result is that while
 350 the NDTRM should more accurately approximate volume fluxes within surfaces of $\bar{\gamma}^{\text{JM97}}$, the NTRM
 351 should more accurately approximate volume fluxes within surfaces of $\bar{\gamma}^{\text{mean}}$. We now test this
 352 prediction using output from an idealized numerical model of the Antarctic continental shelf and
 353 slope. We use this model because its geometry simplifies the task of computing $\bar{\gamma}^{\text{mean}}$, and because
 354 nonlinearities in the seawater equation of state lead to relatively pronounced deviations of potential
 355 density and Neutral Density surfaces in the simulated region [1,37,38].

356 4.1. Model configuration

357 The modeling approach has been described in detail by [1,39–42], so here we present only salient
 358 aspects of its configuration and refer the reader to previously published articles. The MIT general
 359 circulation model [43,44] was configured in a zonally re-entrant channel of length $L_x = 400$ km and
 360 width $L_y = 450$ km, with its depth ranging from 500 m over the continental shelf at the southern
 361 boundary to 3000 m at the northern boundary. The model was forced via a combination of a steady
 362 westward surface wind stress, linear drag at the sea floor, a two-equation representation of surface

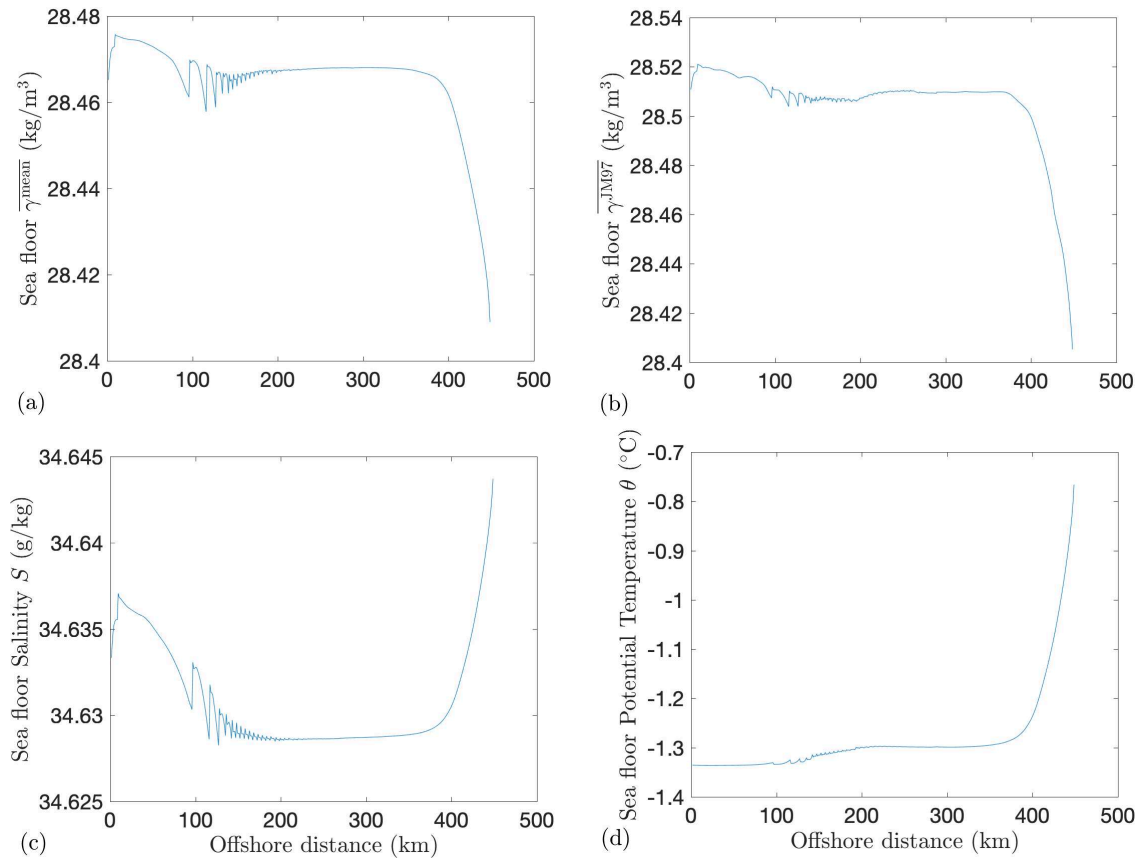


Figure 2. Time-/alongshore-mean (a) γ^{mean} , (b) γ^{J97} , (c) salinity and (d) potential temperature in the bottom-most model grid point, *i.e.* in the layer of dense water that descends down the continental slope [42], as a function of distance from the shore. This plot illustrates that the use of an independent reference dataset leads to a spurious local minima, *e.g.* around $y = 200$ km, in γ^{J97} . These are absent in γ^{mean} , indicating that it more closely tracks Neutral Surfaces. The rapid density variations around $y = 100$ km are due to “steps” in the model’s geopotential-coordinate representation of the continental slope.

363 sea ice heat and salt exchanges [see 42], a constant input of salt over the southernmost 50 km of the
 364 model domain, and restoring toward profiles of θ and S derived from hydrography within a sponge
 365 layer covering the northernmost 50 km of the domain. The model’s horizontal grid spacing is around
 366 1 km, sufficient to resolve the eddy field [41], and the vertical grid consists of 53 vertical levels with
 367 spacings increasing from around 13 m at the surface to around 100 m at the sea floor. The analysis
 368 conducted here uses 5 years of daily model snapshots from a period in which the simulation had
 369 reached statistically steady state.

370 4.2. Constructing Neutral Density from the model’s mean state

371 To test the NTRM we must first construct γ^{mean} , *i.e.* for each time t_n and model grid location
 372 (x_i, y_j, z_k) we must assign Neutral Densities $\gamma^{\text{mean}}(x_i, y_j, z_k, t_n)$, where $i = 1 \dots N_x$, $j = 1 \dots N_y$,
 373 $k = 1 \dots N_z$, and $n = 1 \dots N_t$ are gridpoint indices. Similar to the procedure laid out by [24], we
 374 require a dataset to which the instantaneous model stratification can be referred in order to assign
 375 a γ^{mean} value to each grid point. In [24], this dataset was the hydrographic climatology of [45] and
 376 a corresponding set of neutral density labels on a coarse global grid. Similarly, for the purpose of
 377 constructing γ^{mean} the reference dataset is the model’s time-mean hydrography, $\bar{S}(y_j, z_k)$ and $\bar{\theta}(y_j, z_k)$
 378 (see Fig. 1(a–b)), and a corresponding set of neutral density labels $\gamma_{\text{ref}}^{\text{mean}}(y_j, z_k)$. Note that the reference

379 dataset is approximately independent of x due to the zonally symmetric model geometry and forcing.
 380 The approximate two-dimensionality of the time-mean hydrography also implies that the neutral
 381 helicity of the reference dataset is zero [29]. Taken together with the simply connected model domain,
 382 this implies that Neutral Surfaces are well defined [46].

383 We now outline the procedure for labeling the reference dataset with $\gamma_{\text{ref}}^{\text{mean}}$ and assigning γ^{mean}
 384 values to instantaneous model output. This procedure closely follows that described by [24], to which
 385 the reader is referred for more specific details of the algorithm. We first labeled the northernmost
 386 model water column, $\gamma_{\text{ref}}^{\text{mean}}(y_{N_y}, z_k)$, by setting it equal to $\gamma^{\text{JM97}}(y_{N_y}, z_k)$. Here γ^{JM97} was calculated
 387 from the hydrographic measurements used to restore the model stratification in the offshore sponge
 388 layer, taking the model domain to lie along a slice between (61W,67S) at $y = 0$ and (50.6W,67S) at $y =$
 389 450 km [1]. We then iterated southward through the model water columns, assigning the j^{th} column,
 390 $\{\gamma_{\text{ref}}^{\text{mean}}(y_j, z_k) \mid k = 1 \dots N_z\}$, from the $(j + 1)^{\text{th}}$ column using the form of the discrete neutral relation
 391 (5) given by [24] and linear vertical interpolation. For grid points in the j^{th} column that were denser
 392 or lighter than any grid point in the $(j + 1)^{\text{th}}$ water column, we linearly extrapolated $\gamma_{\text{ref}}^{\text{mean}}(y_j, z_k)$
 393 vertically. Note that in our vertical density extrapolation we assigned the vertical gradient of $\gamma_{\text{ref}}^{\text{mean}}$
 394 to be equal to the vertical gradient of locally-referenced potential density, whereas in this region the
 395 vertical gradient of γ^{JM97} was typically assigned to be twice the vertical gradient of locally-referenced
 396 potential density (the “b-factor” of [24]). This choice of extrapolation was made for simplicity and
 397 should not influence our results, though a consequence is that γ^{mean} spans a smaller range of density
 398 values than γ^{JM97} in this model domain.

399 To calculate $\gamma^{\text{mean}}(x_i, y_j, z_k, t_n)$ for a given model gridpoint with salinity $S(x_i, y_j, z_k, t_n)$
 400 and potential temperature $\theta(x_i, y_j, z_k, t_n)$, we construct continuous functions of z , $\bar{S}(y_j, z)$ and
 401 $\bar{\theta}(y_j, z)$, via linear interpolation. We then find a depth z_r such that $(\bar{S}(y_j, z_r), \bar{\theta}(y_j, z_r), z_r)$
 402 and $(S(x_i, y_j, z_k, t_n), \theta(x_i, y_j, z_k, t_n), z_k)$ satisfy the discrete neutral relation. We then assigned
 403 $\gamma^{\text{mean}}(x_i, y_j, z_k, t_n)$ by linear vertical interpolation of $\gamma_{\text{ref}}^{\text{mean}}(y_j, z_k)$ to the point z_{ref} . Note that our
 404 algorithm for assigning γ^{mean} differs slightly from the algorithm of [24] for assigning γ^{JM97} : to assign
 405 γ^{mean} we refer each gridpoint to a horizontally local “cast” consisting of the Eulerian-mean model
 406 properties, whereas the algorithm of [24] refers each gridpoint to a four geographically local reference
 407 casts. Additionally, we use linear vertical interpolation to assign a γ^{JM97} value, whereas the algorithm
 408 of [24] uses quadratic interpolation.

409 In Fig. 1(a–b) we plot the time- and zonal-mean potential temperature and salinity, $\bar{\theta}$ and \bar{S} , that
 410 serve as the reference dataset in the construction of γ^{mean} . The mean state is qualitatively similar
 411 to hydrographic measurements from the western Weddell Sea [41], and exhibits a layer of relatively
 412 cold, fresh, shelf-sourced bottom water that descends down the continental slope. Fig. 1(c) shows
 413 the time and zonal mean of the Neutral Density constructed from the model’s mean state, *i.e.* $\bar{\gamma}^{\text{mean}}$,
 414 while Fig. 1(d) shows the difference between $\bar{\gamma}^{\text{JM97}}$ and $\bar{\gamma}^{\text{mean}}$. As expected, $\bar{\gamma}^{\text{JM97}}$ takes lower values
 415 than $\bar{\gamma}^{\text{mean}}$ in waters lighter than the lightest water at the northern boundary, and higher values than
 416 $\bar{\gamma}^{\text{mean}}$ in waters denser than the densest water at the northern boundary, due to the procedure for
 417 extrapolating $\gamma_{\text{ref}}^{\text{mean}}$. Some variations are visible across the continental slope due to the presence
 418 of alternating along-slope jets that slowly drift offshore, and which do not perfectly cancel under
 419 integration over the 5-year analysis period [42].

420 We anticipate that γ^{mean} should be more closely aligned with local Neutral Surfaces than γ^{JM97} . To
 421 illustrate this, in Fig. 2 we plot the $\bar{\gamma}^{\text{mean}}$, $\bar{\gamma}^{\text{JM97}}$, $\bar{\sigma}_0$, $\bar{\theta}$ and \bar{S} at the sea floor as a function of cross-slope
 422 distance, *i.e.* within the dense outflowing layer of shelf-sourced bottom water. Fig. 2 shows that $\bar{\gamma}^{\text{JM97}}$
 423 exhibits spurious fluctuations and local minima, on the order of 0.01 kg m^{-3} , that are absent in $\bar{\gamma}^{\text{mean}}$.
 424 For example, around $y = 200$ km there are negligible variations in $\bar{\theta}$ and \bar{S} , indicating that the sea floor
 425 should coincide with a neutral surface. This is reflected in $\bar{\gamma}^{\text{mean}}$, but not in $\bar{\gamma}^{\text{JM97}}$, which exhibits a
 426 spurious local minimum at this point. We conclude that iso-surfaces of γ^{mean} are more closely aligned
 427 with local Neutral Surfaces than γ^{JM97} , though the spurious variations in γ^{JM97} are nonetheless quite
 428 small compared to the domain-scale ranges of γ^{mean} and γ^{JM97} .

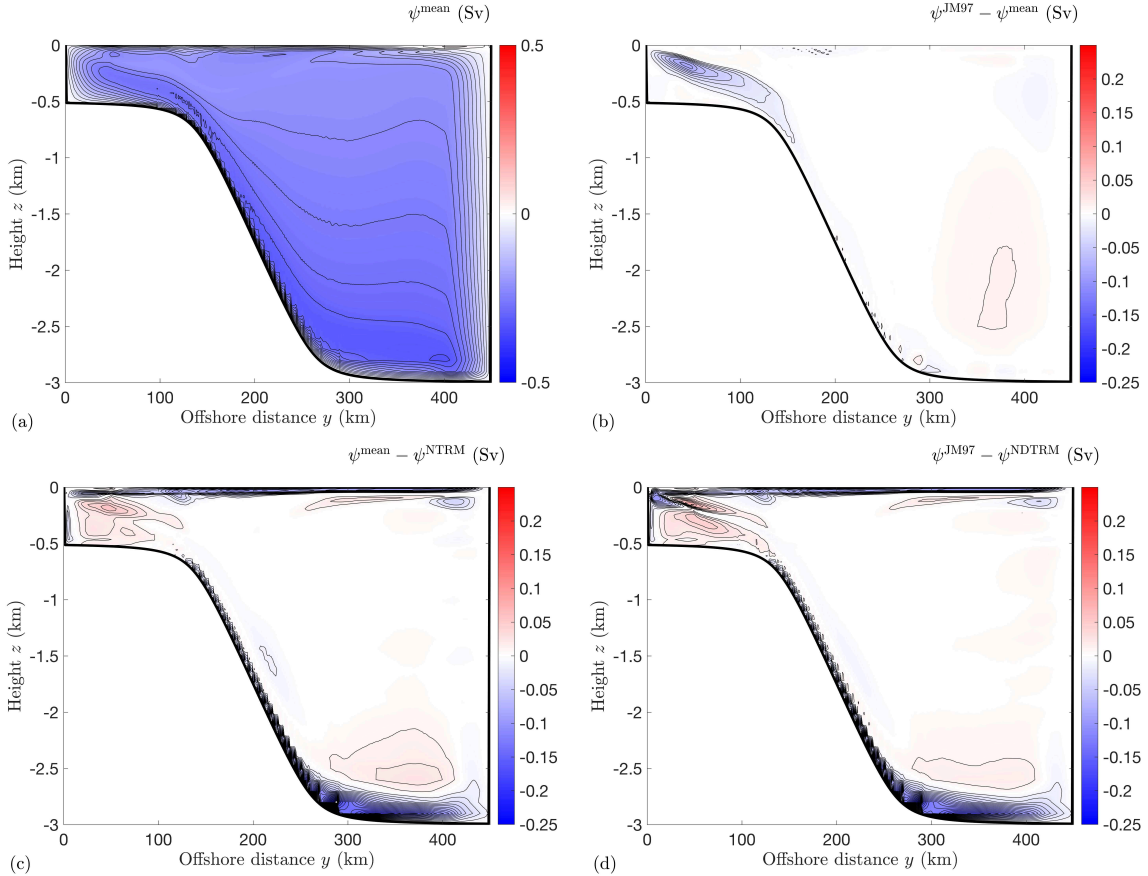


Figure 3. Comparison of transports calculated via TRM approximations vs. diagnosed directly from model output by averaging within density surfaces. Transports are quantified via streamfunctions with blue colors corresponding to counter-clockwise circulation and black contours shown at intervals of (a) 0.025 Sv and (b-d) 0.01 Sv. (a) Diagnosed transport within γ^{mean} surfaces (ψ^{mean}), (b) difference between diagnosed transports within γ^{JM97} surfaces and γ^{mean} surfaces ($\psi^{\text{JM97}} - \psi^{\text{mean}}$), (c) difference between NTRM-estimated transport within γ^{mean} surfaces and diagnosed transport within γ^{mean} surfaces ($\psi^{\text{NTRM}} - \psi^{\text{mean}}$), (d) difference between NDTRM-estimated transport within γ^{mean} surfaces and diagnosed transports within γ^{JM97} surfaces ($\psi^{\text{NDTRM}} - \psi^{\text{JM97}}$). The diagnosed streamfunctions, ψ^{mean} and ψ^{JM97} , have been mapped from density to z coordinates using the time-mean depths of γ^{mean} and γ^{JM97} surfaces, respectively.

429 4.3. Comparing diagnosed and TRM transports

430 Having constructed γ^{mean} , we now compare the transports within γ^{mean} and γ^{JM97} surfaces, as
 431 estimated by the TRM and diagnosed directly from the model simulations. Based on §3, we anticipate
 432 that the NTRM should more closely approximate the diagnosed fluxes within γ^{mean} surfaces, while
 433 the NDTRM should more closely approximate the diagnosed fluxes within γ^{JM97} surfaces.

434 We diagnose fluxes within density surfaces via direct calculation of (1). The procedure is
 435 summarized here to achieve a self-contained presentation; for further details the reader is referred to
 436 ST15. For each model snapshot, the model-reported meridional volume fluxes and Neutral Density
 437 (γ^{mean} or γ^{JM97}) on geopotential surfaces are interpolated to a vertical grid that is 10 times finer than
 438 the model's vertical grid (see [1,41,42]). The volume fluxes are then assigned to a discrete set of
 439 density bins, averaged in time to compute mean volume fluxes within density surfaces, and integrated
 440 vertically in density space to obtain the streamfunction. To map the streamfunction back to z -space,
 441 we also average the height z_0 of each density surface, and map the streamfunction at density γ_0 to

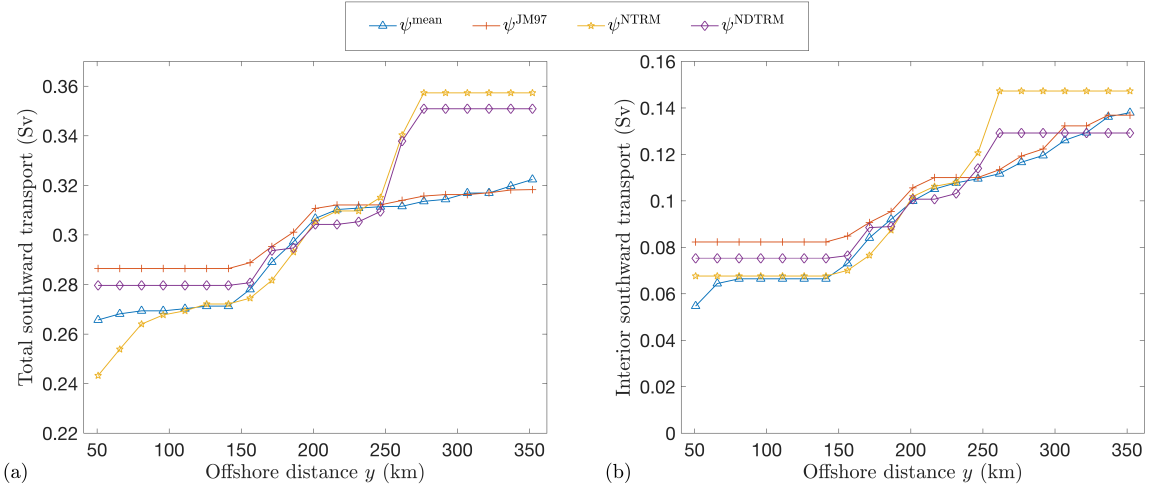


Figure 4. Comparison of total thickness-weighted average cross-slope transports calculated via TRM approximations vs. diagnosed directly from model output. (a) Total southward transport, (b) total interior southward transport, *i.e.* excluding wind-driven Ekman transport of surface waters [see §4 and 1].

height \bar{z}_0 . This allows for direct comparison with the TRM, which approximates the transport above the isopycnal whose mean elevation is \bar{z}_0 . Note that due to the zonal symmetry of the model domain, we only calculate the meridional component of the streamfunction, which quantifies circulation in the y/z plane. We denote the streamfunction corresponding to volume fluxes in γ^{mean} surfaces as ψ^{mean} , and the streamfunction corresponding to volume fluxes in γ^{JM97} surfaces as ψ^{JM97} .

We compare ψ^{mean} and ψ^{JM97} with the NTRM and NDTRM estimates of the volume fluxes. The NTRM is evaluated as the meridional component of (20), with the mean operator defined as a time and zonal average. We denote the resulting streamfunction as ψ^{NTRM} . The NDTRM streamfunction is defined following equation (B.4) of ST15, and is denoted as ψ^{NDTRM} . Throughout this section we use “NDTRM” to refer to the NDTRM2 of ST15, which was shown to exhibit closer agreement with diagnosed fluxes in γ^{JM97} surfaces than lower-order formulations of the NDTRM.

In Fig. 3 we compare ψ^{mean} and ψ^{JM97} , ψ^{NTRM} and ψ^{NDTRM} directly. Fig. 3(a) shows the overturning circulation diagnosed from volume fluxes within γ^{mean} surfaces. The circulation is characterized by wind-driven shoreward transport within the surface mixed layer and shoreward interior eddy transport across the continental slope [42]. These shoreward transports are returned offshore via dense shelf water export down the continental slope. Fig. 3 quantifies the difference in the computed transports within γ^{mean} and γ^{JM97} surfaces. The most substantial difference is that the amplitude of ψ^{JM97} is enhanced relative to ψ^{mean} over the upper continental slope and the continental shelf, exceeding the ~ 0.23 Sv shelf overturning magnitude of ψ^{mean} by around 0.08 Sv. This suggests that a non-negligible fraction of the diagnosed shelf overturning in ψ^{JM97} surfaces is due to errors introduced by the independent reference dataset of [24]. Figs. 3(c-d) show the differences between ψ^{mean} and ψ^{NTRM} , and between ψ^{JM97} and ψ^{NDTRM} , respectively. Both TRM streamfunctions somewhat underestimate the amplitude of the overturning circulation over the continental shelf, and also exhibit errors close to the ocean surface and floor, where the vertical stratification is weak. The latter might be ameliorated by adopting a generalized form of the NTRM that utilizes vertical tracer fluxes in weakly-stratified regions, analogous to the methods proposed by [47,48]. The errors are typically smaller than 0.05 Sv in magnitude, which is smaller than the difference between ψ^{mean} and ψ^{JM97} over the shelf, suggesting that ψ^{NTRM} more closely approximates ψ^{mean} and that ψ^{NDTRM} more closely approximates ψ^{JM97} .

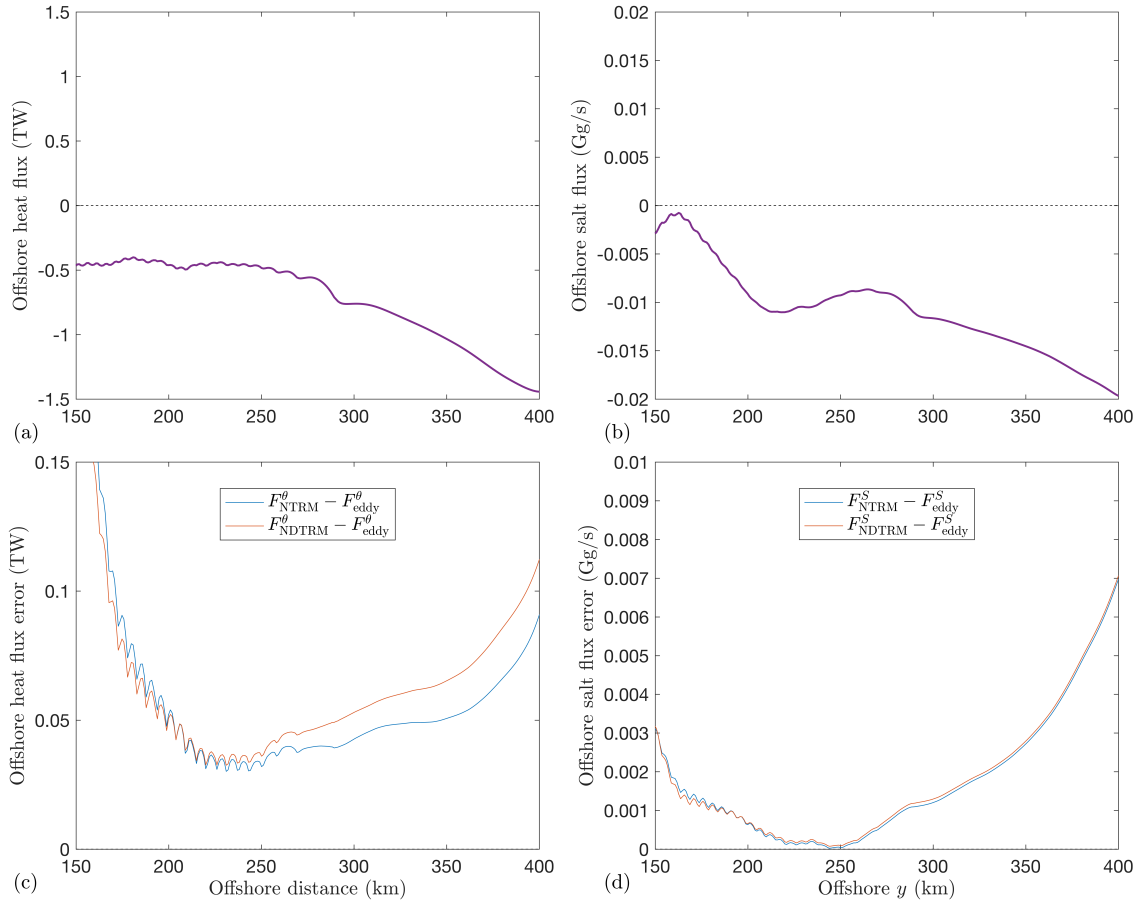


Figure 5. Comparison between cross-slope heat and salt fluxes diagnosed directly from the model output vs. estimated using TRM streamfunctions (see §4). Fluxes are plotted over a subset of the model domain in which the eddy transport was found to be primarily advective, rather than diffusive [42]. (a,b) Diagnosed offshore heat and salt fluxes, respectively. (c,d) Differences between diagnosed and NTRM-/NDTRM-estimated offshore heat and salt fluxes, respectively.

471 To quantify the agreement between the TRM and diagnosed transports, in Fig. 4(a) we compare
 472 the net southward transport reported by each streamfunction, as a function of latitude. This calculation
 473 follows ST15, and only includes southward transport at any given latitude if that transport has been
 474 supplied from the northern boundary of the domain, *i.e.* only counting streamlines that connect
 475 that latitude to the northern boundary. Fig. 4(b) shows a similar comparison, but only accounting
 476 for southward interior transport, *i.e.* excluding transport in the surface mixed layer. In each case,
 477 ψ^{NTRM} and ψ^{NDTRM} more closely tracks ψ^{mean} and ψ^{IM97} , respectively, over the continental slope
 478 ($y \lesssim 150$ km). Over the continental slope ($150 \text{ km} \lesssim y \lesssim 250$ km) the transports are difficult to
 479 distinguish, as suggested by Fig. 3. In the deep ocean ($y \gtrsim 250$ km) the TRM and diagnosed transports
 480 diverge due to large differences in the streamfunctions close to the sea floor (see Fig. 3(c-d)). Thus,
 481 our net southward transport metrics confirm the result suggested by the overturning streamfunction
 482 comparison in Fig. 3: the NTRM more closely approximates volume fluxes in ψ^{mean} surfaces, while the
 483 NDTRM more closely approximates fluxes in ψ^{IM97} surfaces.

484 4.4. Advective tracer transport

485 Finally, we note that that in addition to estimating isopycnal/diapycnal transports, TRM
 486 streamfunctions may also be used to estimate the advective flux of tracers. Importantly, no
 487 globally-defined density variable is needed to perform such an estimate, so, *e.g.*, it would not be

488 necessary to construct a Neutral Density variable like γ^{mean} in conjunction with the NTRM for this
 489 purpose. We now compare the advective meridional fluxes of θ and S estimated by the NTRM and
 490 NDTRM with those diagnosed from the model simulation. We focus on the continental shelf and open
 491 ocean regions ($y \gtrsim 150$ km), in which the heat and salt transports have been shown to be primarily
 492 advective, rather than diffusive [42].

493 Fig. 5(a–b) shows the northward eddy fluxes of heat and salt, diagnosed directly from the daily
 494 model output via

$$495 F_{\text{eddy}}^{\chi} = L_x \int_{-h}^0 \overline{v' \chi'} dz. \quad (37)$$

496 Here $\chi = \theta$ or $\chi = S$, $z = -h(y)$ is the sea floor elevation, the mean operator $\overline{\cdot}$ denotes a time and
 497 zonal average, and primes $'$ denote deviations from that average. The heat and salt fluxes have been
 498 rescaled to take units of TW and Gg/s, respectively, for ease of interpretation. We calculate NTRM
 499 and NDTRM estimates of the advective fluxes via

$$500 F_{\text{TRM}}^{\chi} = -L_x \int_{-h}^0 \frac{\partial \psi_{\text{TRM}}}{\partial z} \overline{\chi} dz. \quad (38)$$

501 Here we set $\psi_{\text{TRM}} = \psi^{\text{NTRM}}$ and $\psi_{\text{TRM}} = \psi^{\text{NDTRM}}$ to define the flux estimates F_{NTRM}^{χ} and F_{NDTRM}^{χ} ,
 502 respectively. In Fig. 5(c–d) we plot the differences between the diagnosed and TRM-estimated heat
 503 and salt fluxes, which typically differ by around 10–20%. There is very little difference between the
 504 NTRM and NDTRM salt fluxes, whereas the NTRM yields errors in the heat flux that are up to 40%
 505 smaller than the errors incurred by using the NDTRM.

506 5. Summary and Conclusion

507 The Temporal Residual Mean (TRM) transport requires an Eulerian approximation for vertical
 508 fluctuations of a set of quasi-material surfaces [e.g. 21–23]. The TRM approximates the transport
 509 within these surfaces, which in turn approximates the semi-Lagrangian mean and Lagrangian-mean
 510 transports [10]. This article builds on a recent study by [1, hereafter ST15], who used the Neutral
 511 Density variable γ^{JM97} of [24] to construct a Neutral Density TRM (NDTRM) that can be applied
 512 anywhere in the ocean, circumventing the limitations of e.g. potential density at high latitudes. A key
 513 result of this article is that the vertical fluctuations of local Neutral Surfaces, which are defined directly
 514 via the continuous form of the neutral relation, can be approximated via (19). The corresponding
 515 TRM streamfunction (20), referred to as the “Neutral TRM” (NTRM) should more closely approximate
 516 the semi-Lagrangian mean transport than the NDTRM, and therefore also better approximate the
 517 generalized Lagrangian mean transport [10]. The NTRM also coincides with a TRM based on vertical
 518 fluctuations of locally-referenced potential density surfaces, again to the same asymptotic order in the
 519 amplitude of the isopycnal height fluctuations.

520 In isolation the NTRM streamfunction does not directly quantify isopycnal and diapycnal ocean
 521 transports [see e.g. 31] because local Neutral Surfaces are, by definition, not globally well-defined.
 522 However, in §3 we showed for the special case of a Neutral Density variable (γ^{mean}) constructed using
 523 the Eulerian-mean ocean state, the NDTRM reduces to the NTRM, up to the same asymptotic order in
 524 the amplitude of the isopycnal height fluctuations. Thus the NTRM approximately quantifies adiabatic
 525 and diabatic volume fluxes within and across γ^{mean} surfaces, again up to a consistent asymptotic order
 526 in the amplitude of the isopycnal height fluctuations.

527 In §4 we tested this theoretical prediction explicitly using an idealized eddy-resolving simulation
 528 of the Antarctic continental shelf and slope. Using the model’s time-mean state as a reference dataset
 529 for γ^{mean} , we labeled the model output with both γ^{mean} and γ^{JM97} and computed volume fluxes within
 530 surfaces of both Neutral Density variables. We showed that γ^{mean} iso-surfaces were more closely
 531 aligned with local Neutral Surfaces than γ^{JM97} , indicating that fluxes within γ^{mean} surfaces should
 532 be more closely aligned with the local neutral tangent plane. Consistent with §3, we found that the
 533 NTRM more closely approximated volume fluxes within γ^{mean} surfaces, while the NDTRM more

534 closely approximated volume fluxes within γ^{JM97} surfaces. Finally, we compared the advective fluxes
535 of heat and salt estimated by the NTRM and NDTRM, with those diagnosed from the model. Both
536 formulations of the TRM yielded flux estimates in close agreement with the diagnosed fluxes, though
537 the NTRM yielded a somewhat closer approximation to the heat fluxes.

538 The results summarized above suggest that for most oceanographic purposes, the NTRM is
539 preferable to the NDTRM for the purposes of estimating isopycnal and diapycnal volume fluxes, and
540 of estimating advective tracer fluxes. It also bears the advantage of being more convenient to compute
541 than the NDTRM, as it makes no explicit reference to globally-defined Neutral Density variable or
542 to the set of reference casts used to define such a variable. A practical consideration is that the
543 NTRM advects a Neutral Density variable constructed from the model's time-mean state, *i.e.* γ^{mean}
544 [23]. Though algorithms for constructing global, approximately neutral density variables have been
545 proposed [*e.g.* 24,49,50], translating these algorithms to the time-mean state of a three-dimensional
546 model with an arbitrary ocean geometry is non-trivial. More recent algorithms have been proposed
547 to construct global, approximately neutral surfaces [46,51], but have not yet been adapted to the
548 construction of three-dimensional Neutral Density variables. Furthermore, a Neutral Density variable
549 such as γ^{mean} would need to be constructed with great care to achieve consistency with γ^{JM97} , which
550 has been used to map the global overturning circulation [6,25].

551 Throughout this manuscript we have assumed that local Neutral Surfaces coincide with purely
552 adiabatic flows [26], and are therefore optimal for the construction of the TRM. Neutral helicity
553 precludes the construction of a continuous density variable that lies exactly parallel to these surfaces
554 everywhere in the ocean [29]. However, on the basis of two-parcel energetic considerations, [52] argued
555 that that adiabatic parcel displacements should not, in fact, follow the neutral tangent plane. Variance
556 of potential temperature and salinity has been found to be larger on Neutral Density surfaces than
557 on surfaces of potential density referenced to 2000 decibars [26,53], though this does not explicitly
558 contradict the notion that adiabatic parcel displacements follow neutral surfaces. Although this topic
559 remains under debate [54–56], an implication is that there may yet be a more accurate choice than
560 local Neutral Surfaces to define adiabatic heaving, and therefore to approximate the semi-Lagrangian
561 mean and generalized Lagrangian mean transports. Further work is required to compare estimates of
562 thickness-weighted average transports within different formulations of quasi-neutral surfaces, such as
563 ω -surfaces [51], thermodynamic neutral density (γ^T) surfaces [50], and orthobaric density surfaces
564 [49].

565 Previous studies have used the NTRM0, and thus implicitly the NTRM (see §3), to estimate
566 volume fluxes within γ^{JM97} surfaces [*e.g.* 42,57–59]. In principle, this incurs an $\mathcal{O}(\tilde{\Delta})$ error in the
567 approximation, where $\tilde{\Delta}$ quantifies differences between the model's mean state and the independent
568 reference dataset. On the other hand, our comparison in §4 shows that the NTRM approximates
569 transports within γ^{JM97} surfaces almost as closely as it approximates transports within γ^{mean} surfaces,
570 so in practice such errors may not be of concern. However, further work is required to evaluate errors
571 associated with neutral helicity when quantifying transports within γ^{mean} surfaces using the NTRM.

572 **Funding:** This material is based in part upon work supported by the National Science Foundation under Grant
573 Numbers OCE-1538702, ANT-1543388 and OCE-1751386.

574 **Acknowledgments:** The author thanks Trevor McDougall and Andrew Thompson for insightful discussions
575 on Neutral Density and the Temporal Residual Mean approximation, and Stefan Riha for many exchanges that
576 played a role in shaping this article. The author also thanks Remi Tallieux, Geoff Stanley and Sjoerd Groeskamp
577 for detailed and insightful reviews that substantially improved the quality of this paper.

578 **Conflicts of Interest:** The author declares no conflicts of interest. The funders had no role in the design of the
579 study; in the collection, analyses, or interpretation of data; in the writing of the manuscript, or in the decision to
580 publish the results.

581

- 582 1. Stewart, A.L.; Thompson, A.F. The Neutral Density Temporal Mean overturning circulation. *Ocean Modelling* **2015**, *90*, 44–56.
- 583 2. Srokosz, M.; Baringer, M.; Bryden, H.; Cunningham, S.; Delworth, T.; Lozier, S.; Marotzke, J.; Sutton, R. Past, present, and future changes in the Atlantic meridional overturning circulation. *Bulletin of the American Meteorological Society* **2012**, *93*, 1663–1676.
- 584 3. Marshall, J.; Speer, K. Closure of the meridional overturning circulation through Southern Ocean upwelling. *Nature Geoscience* **2012**, *5*, 171–180.
- 585 4. Döös, K.; Webb, D.J. The Deacon cell and the other meridional cells of the Southern Ocean. *Journal of Physical Oceanography* **1994**, *24*, 429–442.
- 586 5. Hirst, A.C.; McDougall, T.J. Deep-water properties and surface buoyancy flux as simulated by a z-coordinate model including eddy-induced advection. *J. Phys. Oceanogr.* **1996**, *26*, 1320–1343.
- 587 6. Lumpkin, R.; Speer, K. Global ocean meridional overturning. *Journal of Physical Oceanography* **2007**, *37*, 2550–2562.
- 588 7. Wolfe, C.L.; Cessi, P. Overturning circulation in an eddy-resolving model: The effect of the pole-to-pole temperature gradient. *J. Phys. Oceanogr.* **2009**, *39*, 125–142.
- 589 8. Sun, S.; Eisenman, I.; Stewart, A.L. The influence of Southern Ocean surface buoyancy forcing on glacial-interglacial changes in the global deep ocean stratification. *Geophys. Res. Lett.* **2016**, *43*, 8124–8132.
- 590 9. Sun, S.; Eisenman, I.; Stewart, A.L. Does Southern Ocean surface forcing shape the global ocean overturning circulation? *Geophys. Res. Lett.* **2018**, *45*, 2413–2423.
- 591 10. Eden, C. Relating Lagrangian, residual, and isopycnal means. *Journal of Physical Oceanography* **2012**, *42*, 1057–1064.
- 592 11. Plumb, R.A. Eddy fluxes of conserved quantities by small-amplitude waves. *Journal of the Atmospheric Sciences* **1979**, *36*, 1699–1704.
- 593 12. Marshall, J.; Radko, T. Residual-mean solutions for the Antarctic Circumpolar Current and its associated overturning circulation. *Journal of Physical Oceanography* **2003**, *33*, 2341–2354.
- 594 13. Abernathey, R.; Marshall, J.; Ferreira, D. The dependence of Southern Ocean meridional overturning on wind stress. *J. Phys. Oceanogr.* **2011**, *41*, 2261–2278.
- 595 14. Stewart, A.L.; Hogg, A.M. Reshaping the Antarctic Circumpolar Current via Antarctic Bottom Water Export. *J. Phys. Oceanogr.* **2017**, *47*, 2577–2601.
- 596 15. Nikurashin, M.; Vallis, G. A theory of deep stratification and overturning circulation in the ocean. *J. Phys. Oceanogr.* **2011**, *41*, 485–502.
- 597 16. Nikurashin, M.; Vallis, G. A theory of the interhemispheric meridional overturning circulation and associated stratification. *J. Phys. Oceanogr.* **2012**, *42*, 1652–1667.
- 598 17. Stewart, A.L.; Ferrari, R.; Thompson, A.F. On the importance of surface forcing in conceptual models of the deep ocean. *J. Phys. Oceanogr.* **2014**, *44*, 891–899.
- 599 18. Burke, A.; Stewart, A.L.; Adkins, J.F.; Ferrari, R.; Jansen, M.F.; Thompson, A.F. The glacial mid-depth radiocarbon bulge and its implications for the overturning circulation. *Paleoceanography* **2015**, *30*, 1021–1039.
- 600 19. Watson, A.J.; Vallis, G.K.; Nikurashin, M. Southern Ocean buoyancy forcing of ocean ventilation and glacial atmospheric CO₂. *Nat. Geosci.* **2015**, *8*, 861.
- 601 20. Thompson, A.F.; Stewart, A.L.; Bischoff, T. A multibasin residual-mean model for the global overturning circulation. *J. Phys. Oceanogr.* **2016**, *46*, 2583–2604.
- 602 21. McDougall, T.J.; McIntosh, P.C. The temporal-residual-mean velocity. Part I: Derivation and the scalar conservation equations. *Journal of Physical Oceanography* **1996**, *26*, 2653–2665.
- 603 22. McDougall, T.J.; McIntosh, P.C. The temporal-residual-mean velocity. Part II: Isopycnal interpretation and the tracer and momentum equations. *Journal of Physical Oceanography* **2001**, *31*, 1222–1246.
- 604 23. Wolfe, C.L. Approximations to the ocean's residual circulation in arbitrary tracer coordinates. *Ocean Modelling* **2014**, *75*, 20–35.
- 605 24. Jackett, D.R.; McDougall, T.J. A neutral density variable for the world's oceans. *Journal of Physical Oceanography* **1997**, *27*, 237–263.
- 606 25. Talley, L.D. Closure of the global overturning circulation through the Indian, Pacific, and Southern Oceans: Schematics and transports. *Oceanography* **2013**, *26*, 80–97.

633 26. McDougall, T.J. Neutral surfaces. *Journal of Physical Oceanography* **1987**, *17*, 1950–1964.

634 27. Iselin, C.O. The influence of vertical and lateral turbulence on the characteristics of the waters at mid-depths. *EOS, Transactions American Geophysical Union* **1939**, *20*, 414–417.

635 28. McDougall, T.J.; Groeskamp, S.; Griffies, S.M. On geometrical aspects of interior ocean mixing. *J. Phys. Oceanogr.* **2014**, *44*, 2164–2175.

636 29. McDougall, T.J.; Jackett, D.R. On the helical nature of neutral trajectories in the ocean. *Progress in Oceanography* **1988**, *20*, 153–183.

637 30. Eden, C.; Willebrand, J. Neutral density revisited. *Deep Sea Research Part II: Topical Studies in Oceanography* **1999**, *46*, 33–54.

638 31. Groeskamp, S.; Griffies, S.M.; Iudicone, D.; Marsh, R.; Nurser, A.J.G.; Zika, J.D. The water mass transformation framework for ocean physics and biogeochemistry. *Ann. Rev. Marine Sci.* **2019**, *11*, 271–305.

639 32. Andrews, D.G.; McIntyre, M.E. An exact theory of nonlinear waves on a Lagrangian-mean flow. *Journal of Fluid Mechanics* **1978**, *89*, 609–646.

640 33. Young, W.R. An exact thickness-weighted average formulation of the Boussinesq equations. *Journal of Physical Oceanography* **2012**, *42*, 692–707.

641 34. Groeskamp, S.; Barker, P.M.; McDougall, T.J.; Abernathey, R.P.; Griffies, S.M. VENM: An Algorithm to Accurately Calculate Neutral Slopes and Gradients. *J. Adv. Model. Earth Sy.* **2019**, *11*, 1917–1939.

642 35. Groeskamp, S.; Iudicone, D. The Effect of Air-Sea Flux Products, Shortwave Radiation Depth Penetration, and Albedo on the Upper Ocean Overturning Circulation. *Geophys. Res. Lett.* **2018**, *45*, 9087–9097.

643 36. McIntosh, P.C.; McDougall, T.J. Isopycnal averaging and the residual mean circulation. *Journal of Physical Oceanography* **1996**, *26*, 1655–1660.

644 37. Gill, A.E. Circulation and bottom water production in the Weddell Sea. *Deep Sea Res.* Elsevier, 1973, Vol. 20, pp. 111–140.

645 38. Thompson, A.F.; Stewart, A.L.; Spence, P.; Heywood, K.J. The Antarctic slope current in a changing climate. *Rev. Geophys.* **2018**, *56*, 741–770.

646 39. Stewart, A.L.; Thompson, A.F. Sensitivity of the ocean's deep overturning circulation to easterly Antarctic winds. *Geophys. Res. Lett.* **2012**, *39*.

647 40. Stewart, A.L.; Thompson, A.F. Connecting Antarctic cross-slope exchange with Southern Ocean overturning. *J. Phys. Oceanogr.* **2013**, *43*, 1453–1471.

648 41. Stewart, A.L.; Thompson, A.F. Eddy-mediated transport of warm Circumpolar Deep Water across the Antarctic shelf break. *Geophys. Res. Lett.* **2015**, *42*, 432–440.

649 42. Stewart, A.L.; Thompson, A.F. Eddy generation and jet formation via dense water outflows across the Antarctic continental slope. *J. Phys. Oceanogr.* **2016**, *46*, 3729–3750.

650 43. Marshall, J.; Hill, C.; Perelman, L.; Adcroft, A. Hydrostatic, quasi-hydrostatic, and nonhydrostatic ocean modeling. *J. Geophys. Res. Oceans* **1997**, *102*, 5733–5752.

651 44. Marshall, J.; Adcroft, A.; Hill, C.; Perelman, L.; Heisey, C. A finite-volume, incompressible Navier Stokes model for studies of the ocean on parallel computers. *J. Geophys. Res. Oceans* **1997**, *102*, 5753–5766.

652 45. Levitus, S. Climatological atlas of the world ocean. *NOAA Prof. Pap.* **1982**, *13*.

653 46. Stanley, G.J. Neutral surface topology. *Ocean Modell.* **2019**, *138*, 88–106.

654 47. Held, I.M.; Schneider, T. The surface branch of the zonally averaged mass transport circulation in the troposphere. *J. Atmos. Sci.* **1999**, *56*, 1688–1697.

655 48. Colas, F.; Capet, X.; McWilliams, J.C.; Li, Z. Mesoscale eddy buoyancy flux and eddy-induced circulation in Eastern Boundary Currents. *J. Phys. Oceanogr.* **2013**, *43*, 1073–1095.

656 49. de Szoeke, R.A.; Springer, S.R.; Oxilia, D.M. Orthobaric density: A thermodynamic variable for ocean circulation studies. *Journal of physical oceanography* **2000**, *30*, 2830–2852.

657 50. Tailleux, R. Generalized patched potential density and thermodynamic neutral density: Two new physically based quasi-neutral density variables for ocean water masses analyses and circulation studies. *J. Phys. Oceanogr.* **2016**, *46*, 3571–3584.

658 51. Klocker, A.; McDougall, T.; Jackett, D. A new method for forming approximately neutral surfaces. *Ocean Science* **2009**, *5*, 155–172.

659 52. Tailleux, R. Neutrality versus materiality: A thermodynamic theory of neutral surfaces. *Fluids* **2016**, *1*, 32.

684 53. Van Sebille, E.; Baringer, M.O.; Johns, W.E.; Meinen, C.S.; Beal, L.M.; De Jong, M.F.; Van Aken, H.M.
685 Propagation pathways of classical Labrador Sea water from its source region to 26 N. *J. Geophys. Res.*
686 *Oceans* **2011**, *116*.

687 54. Tailleux, R. On the validity of single-parcel energetics to assess the importance of internal energy and
688 compressibility effects in stratified fluids. *J. Fluid Mech.* **2015**, *767*.

689 55. McDougall, T.; Groeskamp, S.; Griffies, S. Comment on Tailleux, R. Neutrality versus Materiality: A
690 Thermodynamic Theory of Neutral Surfaces. *Fluids* **2016**, *1*, 32. *Fluids* **2017**, *2*, 19.

691 56. Tailleux, R. Reply to “Comment on Tailleux, R. Neutrality Versus Materiality: A Thermodynamic Theory
692 of Neutral Surfaces. *Fluids* **2016**, *1*, 32.”. *Fluids* **2017**, *2*, 20.

693 57. Stewart, A.L.; Klocker, A.; Menemenlis, D. Circum-Antarctic Shoreward Heat Transport Derived From an
694 Eddy-and Tide-Resolving Simulation. *Geophys. Res. Lett.* **2018**, *45*, 834–845.

695 58. Palócz, A.; Gille, S.T.; McClean, J.L. Oceanic heat delivery to the Antarctic continental shelf: Large-scale,
696 low-frequency variability. *J. Geophys. Res. Oceans*, in press **2018**.

697 59. Stewart, A.L.; Klocker, A.; Menemenlis, D. Acceleration and overturning of the Antarctic Slope Current by
698 winds, eddies, and tides. *J. Phys. Oceanogr.* **2019**, *49*, 2043–2074.

699 © 2019 by the authors. Submitted to *Fluids* for possible open access publication under the terms and conditions
700 of the Creative Commons Attribution (CC BY) license (<http://creativecommons.org/licenses/by/4.0/>).